

Higgs mediated Double Flavor Violating top decays in Effective Theories

A. Fernández^(a), C. Pagliarone^(b), F. Ramírez-Zavaleta^(c),
and J. J. Toscano^(a)

^(a)Facultad de Ciencias Físico Matemáticas, Benemérita Universidad Autónoma de Puebla, Apartado Postal 1152, Puebla, Pue., México.

^(b)Università di Cassino & Istituto Nazionale di Fisica Nucleare Pisa, Italy.

^(c)Facultad de Ciencias Físico Matemáticas, Universidad Michoacana de San Nicolás de Hidalgo, Avenida Francisco J. Mújica S/N, 58060, Morelia, Michoacán, México.

Abstract. The possibility of detecting double flavor violating top quark transitions at future colliders is explored in a model-independent manner using the effective Lagrangian approach through the $t \rightarrow u_i \tau \mu$ ($u_i = u, c$) decays. A Yukawa sector that contemplates $SU_L(2) \times U_Y(1)$ invariants of up to dimension six is proposed and used to derive the most general flavor violating and CP violating $q_i q_j H$ and $l_i l_j H$ vertices of renormalizable type. Low-energy data, on high precision measurements, and experimental limits are used to constraint the $t u_i H$ and $H \tau \mu$ vertices and then used to predict the branching ratios for the $t \rightarrow u_i \tau \mu$ decays. It is found that this branching ratios may be of the order of $10^{-4} - 10^{-5}$, for a relative light Higgs boson with mass lower than $2m_W$, which could be more important than those typical values found in theories beyond the standard model for the rare top quark decays $t \rightarrow u_i V_i V_j$ ($V_i = W, Z, \gamma, g$) or $t \rightarrow u_i l^+ l^-$. LHC experiments, by using a total integrated luminosity of 3000 fb^{-1} of data, will be able to rule out, at 95% C.L., DFV top quark decays up to a Higgs mass of $155 \text{ GeV}/c^2$ or discover such a process up to a Higgs mass of $147 \text{ GeV}/c^2$.

PACS numbers: 14.65.Ha, 12.60.Fr, 12.15.Ff, 12.15.Mm

1. Introduction

Despite of the fact that the top quark is the heaviest known particle, with a mass comparable to the electroweak symmetry breaking scale, its dynamical behavior is rather restrictive. For instance, its lifetime is so short that it decays before hadronizing, almost exclusively, into the bW mode. In fact, even though the nondiagonal $t \rightarrow dW$ and $t \rightarrow sW$ decays have sizable branching ratios, they play a quite marginal role compared with the $t \rightarrow bW$ channel. For instance, the $t \rightarrow sW$ decay has a branching ratio of order of 10^{-3} . Rare three-body decays generated at the tree level, as $t \rightarrow d_i W Z$ ($d_i = d, s$) and $t \rightarrow u_i W W$ ($u_i = u, c$) are also severely restricted due to phase space limitations and thus they strongly depend on the precise value of the top mass [1, 2]. At the one-loop level, the interesting flavor changing neutral current (FCNC) decays $t \rightarrow cV$ ($V = \gamma, g, Z, H$) are induced, but they have undetectable branching ratios ranging from 10^{-10} to 10^{-14} [3, 4]. These peculiarities, along with diverse theoretical considerations, suggest that the top quark could be very sensitive to new physics effects, which may manifest themselves through anomalous rates for the top quark production and decay modes. Although some properties of the top quark have already been examined at the Tevatron [5], a further scrutiny is expected at the CERN Large Hadron Collider (LHC), which will operate as a veritable top quark factory, producing about ten millions of $t\bar{t}$ events per year in its first stage, and hopeful up to about eighteen millions in subsequent years [6]. Some complementary studies will be realized at e^+e^- linear colliders [7]. Once operating, many rare processes, involving this particle, are expected to be accessible. It is thus worth investigating some rare top quark decays that are very suppressed within the standard model (SM), as they could constitute windows through which new physics effects may show up.

In this paper, we are interested in the investigation of possible new sources of flavor violation both in the quark and the lepton sectors, through the double flavor violating top quark decay $t \rightarrow u_i \tau^\pm \mu^\mp$, that could affect the SM top dilepton signatures by adding extra leptons or by producing an asymmetry in the ee , $e\mu$, $\mu\mu$, $e\tau$, $\mu\tau$ and $\tau\tau$ + jets final states. Apart from its intrinsic interest, our motivation to study this rare process was triggered from some top quark analysis published, by the CDF Collaboration [8] which revealed some level of asymmetry in the number of ee , $\mu\mu$, and $e\mu$ + jets events, coming from $t\bar{t}$ di-lepton searches, that may be interpreted in terms of such types of rare top quark decays. This decay is very suppressed within the SM, as it occurs at order α^4 through a complicated sequence of subprocesses, namely, $t \rightarrow Wb \rightarrow u_i W W \rightarrow u_i \tau \mu \nu_\tau \nu_\mu$. We will focus on extended Yukawa sectors that are always present within the SM with additional $SU_L(2)$ -Higgs multiplets or in larger gauge groups. Some processes naturally associated with flavor violation or CP violation could be significantly impacted by Yukawa sectors associated with multi-Higgs models, as it is expected that more complicated Higgs sectors tend to favor this class of new physics effects. We will assume that the double flavor violating decay $t \rightarrow u_i \tau \mu$ is mediated by a virtual scalar field with a mass of the order of the Fermi scale $v \approx 246$ GeV. However, instead of tackling the problem in a specific model, we will adopt a model independent approach by using the effective Lagrangian technique [9], which is an appropriate scheme to study those processes that are suppressed or forbidden in the SM. As it has been shown in Refs. [10, 11, 12], it is not necessary to introduce new degrees of freedom in order to generate flavor

‡ From now on, we will use the notation $\tau\mu$ instead of $\tau^\pm\mu^\mp$.

violation at the level of classical action, the introduction of operators of dimension higher than four will be enough. We will see below that an effective Yukawa sector that incorporates $SU_L(2) \times U_Y(1)$ -invariants of up to dimension six is enough to reproduce, in a model independent manner, the main features that are common to extended Yukawa sectors, such as the presence of both flavor violation and CP violation. Although theories beyond the SM require more complicated Higgs sectors that include new physical scalars, we stress that our approach for studying the $t \rightarrow u_i \tau \mu$ decay mediated by a relatively light scalar particle is sufficiently general to incorporate the most relevant aspects of extended theories, as in most cases, it is always possible to identify in an appropriate limit a SM-like Higgs boson whose couplings to pairs of W and Z bosons coincide with those given in the minimal SM. Besides its model independence, our framework has the advantage that it involves an equal or even less number of unknown parameters than those usually appearing in specific extended Yukawa sectors. One important ingredient of our study consists in supporting our predictions, as much as possible, in the available experimental data. For this purpose, in order to predict the branching ratio of the $t \rightarrow u_i \tau \mu$ decay, we will use the current low-energy data to get bounds on the flavor violating Htu_i and $H\tau\mu$ couplings. As we will see below, the best constraint on the Htu_i coupling arises from the recently observed $D^0 - \bar{D}^0$ mixing [13, 14, 15], although the experimental uncertainty on the proton dipole moment provides a lightly lower bound. As to the $H\tau\mu$ coupling, we will see that the best bound arises from the experimental uncertainty on the muon magnetic dipole moment. A less stringent bound for the $H\tau\mu$ coupling is derived from the experimental limit on the branching ratio of the $\tau \rightarrow \mu \bar{\mu} \mu$ decay. We will present explicit expressions that can eventually be used for bounding the parameters of any specific model. Our expression for the branching ratio of the $t \rightarrow u_i \tau \mu$ decay is also of general applicability, as it may be adapted easily to any specific model.

The paper has been organized as follows. In Section 2 the gauge structure of an effective Yukawa sector that include up to dimension-six $SU_L(2) \times U_Y(1)$ -invariant operators is discussed. Section 3 is devoted to calculate the branching ratio for the $t \rightarrow u_i \tau \mu$ decay. In Section 4 a comprehensive analysis concerning the impact of the effective Yukawa sector on low-energy observables is carry out in order to determine the best constraints for the Htu_i and $H\tau\mu$ flavor violating couplings. Section 5 is reserved to present results and analyze the experimental perspectives. Finally, in Section 6 the conclusions are presented.

2. Effective Lagrangian for the Yukawa sector

In the SM the Yukawa sector is both flavor-conserving and CP-conserving, but these effects can be generated at the tree level if new scalar fields are introduced. One alternative, which does not contemplate the introduction of new degrees of freedom, consists in incorporating into the classical action the virtual effects of the heavy degrees by introducing $SU_L(2) \times U_Y(1)$ -invariant operators of dimension higher than four [10, 11]. Indeed, it is only necessary to extend the Yukawa sector with dimension-six operators to induce the most general coupling of the Higgs boson to quarks and leptons. A Yukawa sector with these features has the following structure [10, 11]

$$\mathcal{L}_{eff}^Y = -Y_{ij}^l (\bar{L}_i \Phi l_j) - \frac{\alpha_{ij}^i}{\Lambda^2} (\Phi^\dagger \Phi) (\bar{L}_i \Phi l_j) + H.c.$$

$$\begin{aligned}
& -Y_{ij}^d(\bar{Q}_i\Phi d_j) - \frac{\alpha_{ij}^d}{\Lambda^2}(\Phi^\dagger\Phi)(\bar{Q}_i\Phi d_j) + H.c. \\
& -Y_{ij}^u(\bar{Q}_i\tilde{\Phi}u_j) - \frac{\alpha_{ij}^u}{\Lambda^2}(\Phi^\dagger\Phi)(\bar{Q}_i\tilde{\Phi}u_j) + H.c.,
\end{aligned} \tag{1}$$

where Y_{ij} , L_i , Q_i , Φ , l_i , d_i , and u_i stand for the usual components of the Yukawa matrix, the left-handed lepton doublet, the left-handed quark doublet, the Higgs doublet, the right-handed charged lepton singlet, and the right-handed quark singlets of down and up type, respectively. The α_{ij} numbers are the components of a 3×3 general matrix, which parametrize the details of the underlying physics, whereas Λ is the typical scale of these new physics effects.

After spontaneous symmetry breaking, this extended Yukawa sector can be diagonalized as usual via the unitary matrices $V_L^{l,d,u}$ and $V_R^{l,d,u}$, which correlate gauge states to mass eigenstates. In the unitary gauge, the diagonalized Lagrangian can be written as follows:

$$\begin{aligned}
\mathcal{L}_{eff}^Y = & -\left(1 + \frac{g}{2m_W}H\right)\left(\bar{E}M_lE + \bar{D}M_dD + \bar{U}M_uU\right) \\
& -H\left(1 + \frac{g}{4m_W}H\left(3 + \frac{g}{2m_W}H\right)\right)\left(\bar{E}\Omega^lP_RE + \bar{D}\Omega^dP_RD\right. \\
& \left. + \bar{U}\Omega^uP_RU + H.c.\right),
\end{aligned} \tag{2}$$

where the M_a ($a = l, d, u$) are the diagonal mass matrix and $\bar{E} = (\bar{e}, \bar{\mu}, \bar{\tau})$, $\bar{D} = (\bar{d}, \bar{s}, \bar{b})$, and $\bar{U} = (\bar{u}, \bar{c}, \bar{t})$ are vectors in the flavor space. In addition, Ω^a are matrices defined in the flavor space through the relation:

$$\Omega^a = \frac{1}{\sqrt{2}}\left(\frac{v}{\Lambda}\right)^2 V_L^a \alpha^a V_R^{a\dagger}. \tag{3}$$

To generate Higgs-mediated FCNC effects at the level of classical action, it is assumed that neither $Y^{l,d,u}$ nor $\alpha^{l,d,u}$ are diagonalized by the $V_{L,R}^a$ rotation matrices, which should only diagonalize the sum $Y^{l,d,u} + \alpha^{l,d,u}$. As a consequence, mass and interactions terms would not be simultaneously diagonalized as it occurs in the dimension-four theory. In addition, if $\Omega^{a\dagger} \neq \Omega^a$, the Higgs boson couples to fermions through both scalar and pseudoscalar components, which in turn could lead to CP violation in some processes. As a consequence, the flavor violating coupling $\bar{f}_i f_j H$, with f stands for a charged lepton [16] or quark, has the most general renormalizable structure of scalar and pseudoscalar type given by §:

$$-i(\Omega_{ij}P_R + \Omega_{ij}^*P_L) = -i[Re(\Omega_{ij}) + iIm(\Omega_{ij})\gamma_5]. \tag{4}$$

To close this section, let us to emphasize that the above effective Lagrangian describes the most general renormalizable coupling of scalar field to pairs of fermions, which reproduces the main features of most of the extended Yukawa sectors. It includes the most general version of the two-Higgs doublet model (THDM-III) [18] and multi-Higgs models that comprise additional multiplets of $SU_L(2) \times U_Y(1)$ or scalar representations of larger gauge groups. Our approach also cover more exotic formulations of flavor violation, as the so-called familons models [19] or theories that

§ The flavor violating coupling $\bar{f}_i f_j H$ can also be induced by $\bar{D}_\mu \bar{F}_i f_{Rj} D^\mu \Phi$ operators, with D_μ the electroweak covariant derivative and F and f stand for doublet and singlet, respectively. However, they would have a marginal role in flavor physics, as this class of operators only may be generated at the one-loop level by the fundamental theory and are thus suppressed with respect to the Yukawa type ones, which can be generated at the tree level [17]. In addition, these operators induce also the $Zf_i f_j$ coupling, allowing us to constraint it through Z physics data [11].

involves an Abelian flavor symmetry [20]. In this way, our results will be applicable to a wide variety of models that predict scalar-mediated flavor violation.

3. The decay $t \rightarrow u_i \tau \mu$

We now proceed to calculate the branching ratio for the $t \rightarrow u_i \tau \mu$ decay using the general couplings for $t u_i H$ and $H \tau \mu$ given in the previous section. This decay occurs through the diagram shown in Figure 1. The amplitude can be written as the product of the amplitudes associated with the subprocesses $t \rightarrow u_i H$ and $H \rightarrow \tau \mu$:

$$\mathcal{M}(t \rightarrow u_i \tau \mu) = \frac{\mathcal{M}(t \rightarrow u_i H) \mathcal{M}(H \rightarrow \tau \mu)}{m^2 - m_H^2 + i m_H \Gamma_H}, \quad (5)$$

where m is the invariant mass of the final state $\tau \mu$ and Γ_H is the total Higgs decay width. Once squared the amplitude, averaging over the top spin states, and introducing a factor of 2 to take into account the two final states $\tau^+ \mu^-$ and $\tau^- \mu^+$, one obtains

$$|\bar{\mathcal{M}}(t \rightarrow u_i \tau \mu)|^2 = \frac{|\bar{\mathcal{M}}(t \rightarrow u_i H)|^2 |\mathcal{M}(H \rightarrow \tau \mu)|^2}{m_t^4 ((x-y)^2 + yz)}, \quad (6)$$

where we have introduced the dimensionless variables $x = m^2/m_t^2$, $y = m_H^2/m_t^2$, and $z = \Gamma_H^2/m_t^2$. In addition, the squared subamplitudes are given by

$$|\bar{\mathcal{M}}(t \rightarrow u_i H)|^2 = m_t^2 \left((1-x) |\Omega_{u_i t}|^2 + 4 \left(\frac{m_{u_i}}{m_t} \right) \text{Re}(\Omega_{u_i t}^2) \right), \quad (7)$$

$$|\mathcal{M}(H \rightarrow \tau \mu)|^2 = m_t^2 \left(x |\Omega_{\tau \mu}|^2 + 4 \left(\frac{m_\tau}{m_t} \right) \left(\frac{m_\mu}{m_t} \right) \text{Re}(\Omega_{\tau \mu}^2) \right). \quad (8)$$

From now on, the masses m_{u_i} and m_μ will be ignored with respect to m_t and m_H , in phase space manipulations. In this approach, the branching ratio for this decay can be written as follows:

$$\text{Br}(t \rightarrow u_i \tau \mu) = \frac{|\Omega_{u_i t}|^2 |\Omega_{\tau \mu}|^2}{256 \pi^3} \left(\frac{m_t}{\Gamma_t} \right) f(y, z), \quad (9)$$

where Γ_t is the top total decay width and

$$f(y, z) = \int_0^1 dx \frac{x(1-x)^2}{(x-y)^2 + yz}. \quad (10)$$

This integral has analytical solution, which is given by

$$\begin{aligned} f(y, z) = & 2y - \frac{3}{2} + \frac{1}{2} \left(3y^2 - (4+z)y + 1 \right) \log \left(\frac{y^2 + (z-2)y + 1}{y(y+z)} \right) \\ & + \sqrt{\frac{y}{z}} \left(y^2 - (2+3z)y + 2z + 1 \right) \left(\tan^{-1} \sqrt{\frac{y}{z}} \right. \\ & \left. + \tan^{-1} \left(\frac{1-y}{\sqrt{yz}} \right) \right). \end{aligned} \quad (11)$$

In order to make predictions, we need to use some values for the $\Omega_{u_i t}$ and $\Omega_{\tau \mu}$ parameters. This is the subject of the next section.

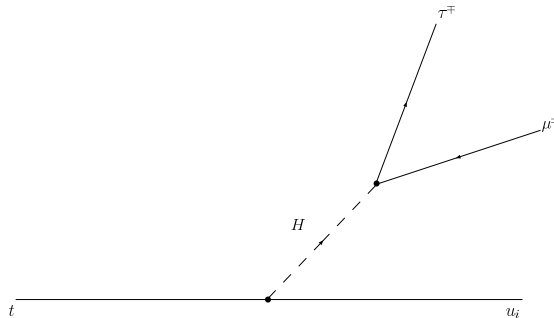


Figure 1. Diagram for double flavor violating top quark decay.

4. Bounding the Htu_i and $H\tau\mu$ vertices from low-energy data

Our goal in this section is to estimate the size of the Ω_{u_it} and $\Omega_{\tau\mu}$ parameters. Although they have already been estimated before by means of the Cheng-Sher ansatz [21] or other similar assumptions [10], in this work, as emphasized in the introduction, we will resort to the available low-energy data. It is obvious that a constraint on the Ω_{u_it} parameter from low-energy data only can be obtained through one-loop or higher order effects. In this case, we will examine the simultaneous one-loop contribution of the Htu and Htc vertices to the mass difference ΔM_D in $D^0 - \overline{D^0}$ mixing recently observed by the Babar [13] and Belle [14] collaborations. Also, the one-loop contribution of the Htu vertex to the magnetic and electric dipole moments of the proton and the neutron will be examined. The contribution of the Htc vertex to these observables would require to consider two-loop effects. However, as we will discuss below, the constraint thus obtained is not appropriated to make predictions. As far as the $\Omega_{\tau\mu}$ parameter is concerned, there are two possible type of processes that eventually could lead to good constraints. These processes are the experimental uncertainty on the muon anomalous magnetic moment and the experimental limits on the lepton flavor violating decays $l_i \rightarrow l_j \bar{l}_k l_k$ and $l_i \rightarrow l_j \gamma$. We will see below that in this case the experimental uncertainty on the muon anomalous magnetic moment provides the best constraint.

4.1. Bounding $\Omega_{tu}\Omega_{tc}$ from $D^0 - \overline{D^0}$ mixing

Recently, the Babar [13] and Belle [14] collaborations have observed signals of $D^0 - \overline{D^0}$ mixing. The Heavy Flavor Averaging Group [15] interpretation of the current data leads to a mass difference of $D^0 - \overline{D^0}$ given by $\Delta M_D = (1.4 \pm 0.5) \times 10^{-15} \text{ GeV}/c^2$. Although this measurement is recent and fluctuations from future refinements can be expected, analysis carried out show that this value is consistent with the SM prediction [22]. In Ref. [22], diverse scenarios of new physics contributions to D mixing are studied. Here, we will investigate the impact of the Htc and Htu vertices on the mass difference ΔM_D . This contributions occurs through the short distance effect characterized by the box diagrams shown in Fig.2. The amplitude is entirely governed by the top and Higgs masses, so we will work in the limit of external masses and momenta equal to zero. In this approximation, the amplitude can be written as

follows

$$\Gamma = 2\Omega_{tu}^2\Omega_{tc}^2 \int \frac{d^4k}{(2\pi)^4} \frac{(\bar{u}(\not{k} + m_t)c)(\bar{u}(\not{k} + m_t)c)}{(k^2 - m_t^2)^2(k^2 - m_H^2)^2}, \quad (12)$$

where the Ω_i parameters have been assumed reals. Notice that the amplitude is free of ultraviolet divergences. Once introduced a Feynman parametrization, the amplitude can be written in the following form

$$\Gamma = -\frac{i}{16\pi^2} \frac{\Omega_{tu}^2\Omega_{tc}^2}{m_t^2} \left(f(x)(\bar{u}\gamma_\mu c)(\bar{u}\gamma^\mu c) + g(x)(\bar{u}c)(\bar{u}c) \right), \quad (13)$$

where $f(x)$ and $g(x)$ ($x = m_H^2/m_t^2$) are the loop functions in the heavy internal mass limit, which are given by

$$f(x) = \frac{1}{2} \frac{1}{(1-x)^3} (1 - x^2 + 2x \log x), \quad (14)$$

$$g(x) = \frac{4}{(1-x)^3} \left(2(1-x) + (1+x) \log x \right), \quad (15)$$

where $f(1) = 1/6$ and $g(1) = -2/3$. The Γ amplitude corresponds to the vertex function associated with the following four-quark effective interaction:

$$\mathcal{L}_{eff} = -\frac{\Omega_{tu}^2\Omega_{tc}^2}{64\pi^2 m_t^2} \left(f(x)(Q_1 + 2Q_2 + Q_6) + g(x)(Q_3 + 2Q_4 + Q_7) \right), \quad (16)$$

where a factor of $1/4$ was introduced in order to compensate two Wick contractions. Here, the Q_i are dimension-six fermionic operators, which are already known in the literature [22]:

$$Q_1 = (\bar{u}_L\gamma_\mu c_L)(\bar{u}_L\gamma^\mu c_L), \quad (17)$$

$$Q_2 = (\bar{u}_L\gamma_\mu c_L)(\bar{u}_R\gamma^\mu c_R), \quad (18)$$

$$Q_6 = (\bar{u}_R\gamma_\mu c_R)(\bar{u}_R\gamma^\mu c_R), \quad (19)$$

$$Q_3 = (\bar{u}_L c_R)(\bar{u}_R c_L), \quad (20)$$

$$Q_4 = (\bar{u}_R c_L)(\bar{u}_R c_L), \quad (21)$$

$$Q_7 = (\bar{u}_L c_R)(\bar{u}_L c_R). \quad (22)$$

On the other hand, the D mass difference is given by

$$\Delta M_D = \frac{1}{M_D} \text{Re} \langle \bar{D}^0 | \mathcal{H}_{eff} = -\mathcal{L}_{eff} | D^0 \rangle, \quad (23)$$

which in our case takes the form

$$\begin{aligned} \Delta M_D &= \frac{\Omega_{tu}^2\Omega_{tc}^2}{64\pi^2} \frac{1}{m_t^2 M_D} \left(f(x) \langle Q_1 \rangle + 2 \langle Q_2 \rangle + \langle Q_6 \rangle \right) \\ &\quad + g(x) (\langle Q_3 \rangle + 2 \langle Q_4 \rangle + \langle Q_7 \rangle) \\ &= \frac{\Omega_{tu}^2\Omega_{tc}^2}{64\pi^2} \left(\frac{f_D}{m_t} \right)^2 \left(\frac{M_D}{12} \right) \left(f(x)(8B_1 - 20B_2 + 8B_6) \right. \\ &\quad \left. + g(x)(7B_3 - 10B_4 - 5B_7) \right), \end{aligned} \quad (24)$$

where the expressions for $\langle Q_i \rangle$ given in Ref. [22] were used. Here, f_D is the D decay constant. We will use the CLEO Collaboration determination $f_D = 222.6 \pm 16.7$ MeV/ c^2 [23]. The factors B_i are unknown, but lattice calculation [24] leads to

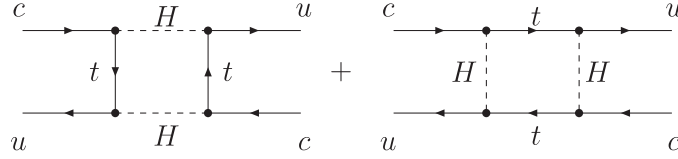


Figure 2. Box diagrams contributing to the $D^0 - \bar{D}^0$ mixing.

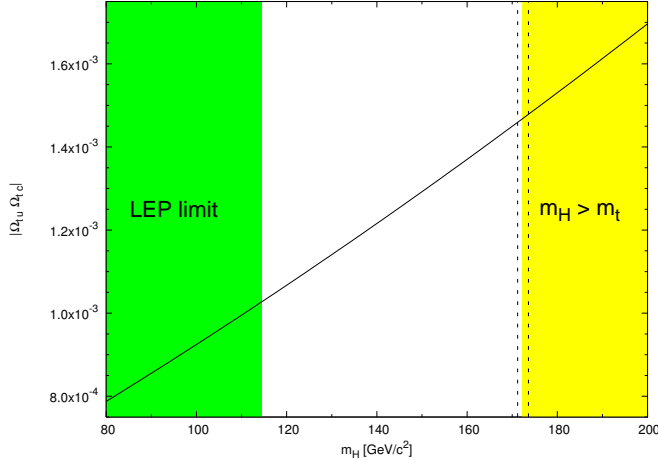


Figure 3. Behavior of $\Omega_{tc}\Omega_{tu}$ with the Higgs mass. The dashed lines represent the current experimental uncertainty on the top quark mass measurement [25].

$B_i \approx 0.8$ [22], although in vacuum saturation and in the heavy quark limit they approximate to the unity. In our numerical analysis, we will use $B_i = 1$. Using the value $M_D = 1.8646 \text{ GeV}/c^2$ [25], one obtains

$$\Delta M_D = 1.6 \times 10^{-9} (f(x) - 2g(x)) \Omega_{tu}^2 \Omega_{tc}^2. \quad (25)$$

To bound the $\Omega_{tu}\Omega_{tc}$ product, we demand that the above contribution does not exceed the experimental uncertainty [13, 14, 15], which leads to

$$|\Omega_{tu}\Omega_{tc}| < \frac{1.8 \times 10^{-3}}{\sqrt{F(x)}}, \quad (26)$$

where $F(x) = f(x) - 2g(x)$. In Figure 3 we show the behavior of $|\Omega_{tu}\Omega_{tc}|$ as a function of the Higgs mass. From this figure, it can be appreciated a moderate variation of $|\Omega_{tu}\Omega_{tc}|$, which go from 0.8×10^{-3} to 1.6×10^{-3} for m_H ranging from $80 \text{ GeV}/c^2$ to $200 \text{ GeV}/c^2$.

4.2. Bounds from flavor diagonal low-energy processes

In this paragraph we will calculate the contribution of the $H f_i f_j$ vertex to the magnetic and electric dipole moments of the f_i fermion, which is given through the diagram shown in Figure 6. In order to have some idea about the importance of the imaginary part of the Ω_{ij} parameter, we will proceed as general as possible, which means that the contribution to both the magnetic and electric dipole moments of f_i will be calculated.

Here, the f_i fermion stands for a light quark or charged lepton. The amplitude for the on-shell $f_i f_j \gamma$ vertex can be written as follows:

$$\mathcal{M} = \bar{u}(p_2) \Gamma_\mu u(p_1) \epsilon^{*\mu}(q, \lambda), \quad (27)$$

where the vertex function is given by

$$\Gamma_\mu = e Q_j \int \frac{d^D k}{(2\pi)^D} \frac{T_\mu}{\Delta}, \quad (28)$$

with

$$T_\mu = |\Omega_{ij}|^2 \left((\not{k} + \not{p}_2) \gamma_\mu (\not{k} + \not{p}_1) + m_j^2 \gamma_\mu \right) + m_j \left(\text{Re}(\Omega_{ij}^2) + i \text{Im}(\Omega_{ij}^{*2}) \gamma_5 \right) (2k_\mu + \not{p}_2 \gamma_\mu + \gamma_\mu \not{p}_1), \quad (29)$$

$$\Delta = [k^2 - m_H^2][(k + p_1)^2 - m_j^2][(k + p_2)^2 - m_j^2]. \quad (30)$$

In the above expressions, Q_j is the electric charge of the internal f_j fermion in units of the positron charge. After using the well known Gordon's identities, it is easy to see that there are contributions to the monopole $[F(q^2)\gamma_\mu]$, the magnetic dipole moment $[i(a_i/2m_i)\sigma_{\mu\nu}q^\nu]$, and the electric dipole moment $(-d_i\gamma_5\sigma_{\mu\nu}q^\nu)$. The contribution to the monopole is divergent, but we only are interested in the magnetic and electric dipole moments, for which the contribution is free of ultraviolet divergences. After some algebra, the form factors associated with the electromagnetic dipoles of f_i can be written as follows:

$$a_i = -\frac{Q_j x_i^2}{8\pi^2} \left(|\Omega_{ij}|^2 f(x_i, x_j) + \left(\frac{x_j}{x_i}\right) \text{Re}(\Omega_{ij}^2) g(x_i, x_j) \right), \quad (31)$$

$$d_i = -\frac{Q_j x_j}{16\pi^2} \left(\frac{e}{m_H}\right) \text{Im}(\Omega_{ij}^2) g(x_i, x_j), \quad (32)$$

where

$$f(x_i, x_j) = \int_0^1 dx \int_0^{1-x} dy \frac{(1-x-y)(x+y)}{R}, \quad (33)$$

$$g(x_i, x_j) = \int_0^1 dx \int_0^{1-x} dy \frac{(x+y)}{R}, \quad (34)$$

with

$$R = 1 - x - y - x_i^2(1-x-y)(x+y) + x_j^2(x+y). \quad (35)$$

In the above expressions the dimensionless variable $x_a = m_a/m_H$ has been introduced. The solutions of these integrals are quite complicated, but we can take $x_i = 0$ in R to obtain simple analytical expressions, which is possible since $x_i \ll x_j$ for all the cases that will be considered here, namely, $m_i = m_u, m_d, m_\mu$. So in this approximation, one obtains

$$f(x_j) = \frac{2 + x_j^2(x_j^4 - 6x_j^2 + 3) + 6x_j^2 \log(x_j^2)}{6(x_j^2 - 1)^4}, \quad (36)$$

$$g(x_j) = \frac{3 + x_j^2(x_j^2 - 4) + 2\log(x_j^2)}{2(x_j^2 - 1)^3}. \quad (37)$$

A simple numerical evaluation shows that $f(x_j)$ is suppressed with respect to $g(x_j)$ by about one order of magnitude. Consequently, the $x_i^2 f(x_j)$ term can be neglected

in the expression for a_i , as it is irrelevant compared with $x_i x_j g(x_j)$. After these considerations, we can write

$$a_i = -\frac{Q_j x_i x_j}{8\pi^2} \text{Re}(\Omega_{ij}^2) g(x_j), \quad (38)$$

$$d_i = -\frac{Q_j x_j}{16\pi^2} \left(\frac{e}{m_H}\right) \text{Im}(\Omega_{ij}^2) g(x_j). \quad (39)$$

Notice that $\text{Re}(\Omega_{ij}^2) = [\text{Re}(\Omega_{ij})]^2 - [\text{Im}(\Omega_{ij})]^2$, which means that the scalar (pseudoscalar) component of the $H f_i f_j$ vertex gives a positive (negative) contribution to the magnetic dipole moment of the fermion in consideration, a fact that is well known from the abundant literature on the muon's anomalous magnetic moment.

We now are in position of using low-energy data to bound the Ω_{tu} and $\Omega_{\tau\mu}$ parameters.

4.2.1. Bounding Ω_{tu} from proton and neutron physics To bound $\text{Re}(\Omega_{tu}^2)$ we can use the available precision measurements on the magnetic dipole moments of the proton and the neutron. We will use the experimental uncertainty on the proton magnetic dipole, as it is the most restrictive. Thus, the contribution of the tuH vertex must be less than this uncertainty, which is given by [25]

$$|\Delta a_p^{Exp}| < 2.8 \times 10^{-8}. \quad (40)$$

As far as $\text{Im}(\Omega_{tu}^2)$ is concerned, we can constraint it using the very stringent experimental limit for the neutron electric dipole moment. The current limit is given by [26]:

$$|d_n| < 2.9 \times 10^{-26} \text{ e.cm}. \quad (41)$$

On the other hand, the magnetic and electric dipole moments of p and n , respectively, are related with those of their elementary constituents through the following expressions

$$a_p = \frac{2}{3}a_u - \frac{1}{3}a_d - \frac{1}{3}a_s, \quad (42)$$

$$d_n = \frac{4}{3}d_d - \frac{1}{3}d_u. \quad (43)$$

We will assume the new physics contributions to a_p and d_n as arising exclusively from the quark u , as in this case $f_j = t$. Also, as usual, we will use $m_d \approx m_u \approx m_n/3 \approx m_p/3$. With these considerations, we can write the following inequalities for the unknown parameters $\text{Re}(\Omega_{tu}^2)$ and $\text{Im}(\Omega_{tu}^2)$:

$$|\text{Re}(\Omega_{tu}^2)| < (54\pi^2) \left| \frac{\Delta a_p^{Exp}}{x_t x_p g(x_t)} \right|, \quad (44)$$

$$|\text{Im}(\Omega_{tu}^2)| < (36\pi^2) \left(\frac{m_H}{e}\right) \left| \frac{d_n^{Exp}}{x_t g(x_t)} \right|. \quad (45)$$

Before analyzing more carefully the behavior of these parameters with the Higgs mass, let us to estimate their size for a given value of m_H . For instance, making $m_H = 100 \text{ GeV}/c^2$, a straightforward evaluation shows that $|\text{Re}(\Omega_{tu}^2)| \lesssim 6 \times 10^{-3}$, whereas $|\text{Im}(\Omega_{tu}^2)| \lesssim 10^{-7}$, which means that the imaginary part of Ω_{tu} is more suppressed

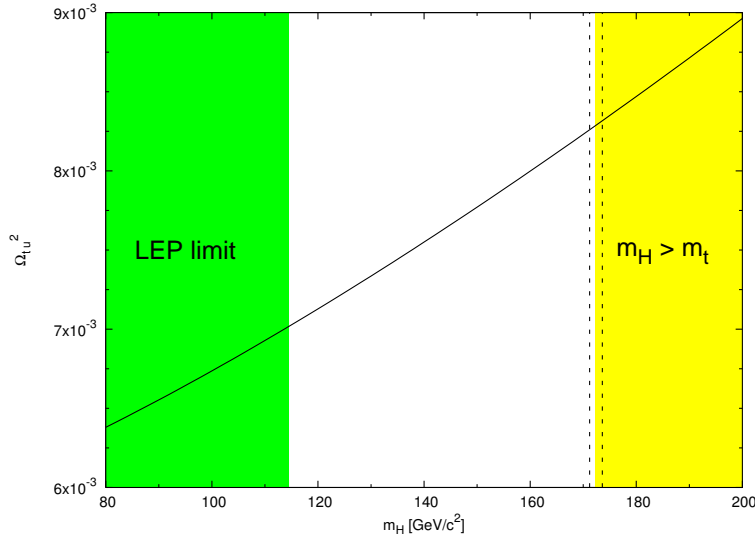


Figure 4. Behavior of Ω_{tu}^2 as a function of the Higgs mass.

than the real part. In the following, we will assume that $Im(\Omega_{tu}) \ll Re(\Omega_{tu})$ or that the Yukawa sector is CP-conserving. After these considerations, we can write

$$\Omega_{tu}^2 < (54\pi^2) \left| \frac{\Delta a_p^{Exp}}{x_t x_p g(x_t)} \right|. \quad (46)$$

In Figure 4, we show the behavior of this parameter as a function of the Higgs mass. From this figure, it can be seen that Ω_{tu}^2 is practically insensitive to the variation of the Higgs mass, as it goes from 6×10^{-3} to 9×10^{-3} for m_H ranging from 80 GeV to 200 GeV/ c^2 .

Having obtained a bound for the Htu vertex, we turn to comment about the difficulties encountered in deriving a constraint on the Htc vertex. This vertex, in contrast with the Htu one, has a less direct connection with the electromagnetic properties of the proton and the neutron, as it contributes to these quantities up to the two-loop level. Due to the presence of the extra loop factor $1/16\pi^2$, a factor proportional to α , and the CKM factor $|V_{cd}|^2$, the two-loop contribution of this coupling to the $dd\gamma$ vertex is severely suppressed, which leads to bounds for $|\Omega_{tc}|$ of about 10^2 . Definitively, it is not possible to obtain an acceptable bound from low-energy data for $|\Omega_{tc}|$, although from general considerations one could expect that it is less restricted than $|\Omega_{tu}|$. In this work, we will adopt a more conservative point of view by assuming that $|\Omega_{tc}|$ obeys the same constraint than $|\Omega_{tu}|$. Since the m_u and m_c masses will be ignored through the calculations, it will not be possible to distinguish among themselves the transitions $t \rightarrow u\tau\mu$ and $t \rightarrow c\tau\mu$. Although our results would be more appropriated for the former of these decays, in the following we will use the notation $t \rightarrow u_i\tau\mu$. Notice that the bound for Ω_{tu_i} derived from the proton magnetic dipole moment is about one order of magnitude less stringent than that obtained from the $D^0 - \bar{D}^0$ mixing.

It is worth comparing our results derived from low-energy data with those that can be obtained from the Cheng-Sher ansatz [21], frequently used to make predictions

in specific flavor violating extended Yukawa sectors. According this ansatz, the size of the Htu_i vertex can be estimated by using the relation $\lambda_{tu_i} \sqrt{m_t m_{u_i}}/v$. Assuming λ_{tu_i} of $O(1)$, one can estimate the values 3×10^{-3} and 6×10^{-2} for the Htu and Htc vertices, respectively. It is interesting to see that our bound for the Htu_i vertex is of the same order of magnitude than that obtained from the Cheng-Sher ansatz for Htc .

4.2.2. Bounding $\Omega_{\tau\mu}$ from muon physics The anomalous magnetic moment of the muon is at present one of the physical observables best measured. Here, we will use the experimental uncertainty on this quantity to impose a bound on $Re(\Omega_{\tau\mu}^2)$. We will assume that the one-loop contribution of the $H\tau\mu$ vertex is less than the experimental uncertainty on this quantity, which is given by [25]:

$$|\Delta a_\mu^{Exp}| < 5.4 \times 10^{-10}. \quad (47)$$

As far as $Im(\Omega_{\tau\mu}^2)$ is concerned, we can use the existing experimental limit on the muon electric dipole moment, which is given by [25]:

$$|d_\mu^{Exp}| < 3.7 \times 10^{-19} \text{ e.cm}. \quad (48)$$

From expressions given by Eqs.(31) and (32), one can write

$$|Re(\Omega_{\tau\mu}^2)| < (8\pi^2) \left| \frac{\Delta a_\mu^{Exp}}{x_\tau x_\mu g(x_\tau)} \right|, \quad (49)$$

$$|Im(\Omega_{\tau\mu}^2)| < (16\pi^2) \left(\frac{m_H}{e} \right) \left| \frac{d_\mu^{Exp}}{x_\tau g(x_\tau)} \right|. \quad (50)$$

The evaluation of these expressions for $m_H = 100 \text{ GeV}/c^2$ leads to $|Re(\Omega_{\tau\mu}^2)| \lesssim 3 \times 10^{-4}$ and $|Im(\Omega_{\tau\mu}^2)| \lesssim 2$, showing that in this case the imaginary part of $\Omega_{\tau\mu}$ is less constrained than the real one. In order to simplify the analysis as much as possible, we will assume that the leptonic Yukawa sector is also CP-conserving. With these assumptions, we can write

$$\Omega_{\tau\mu}^2 < (8\pi^2) \left| \frac{\Delta a_\mu^{Exp}}{x_\tau x_\mu g(x_\tau)} \right|. \quad (51)$$

In Figure 5, the behavior of $\Omega_{\tau\mu}^2$ as a function of m_H is shown. From this figure, it can be seen that $\Omega_{\tau\mu}^2$ varies in approximately one order of magnitude in the interval $80 \text{ GeV}/c^2 < m_H < 200 \text{ GeV}/c^2$.

4.3. Bounds from lepton flavor violating transitions

In this subsection, we explore the possibility of deriving a bound for the $H\tau\mu$ vertex from nondiagonal lepton transitions [27]. The best candidates are the $\tau \rightarrow \mu\bar{\mu}\mu$ and $\tau \rightarrow \mu\gamma$ decays, to which there exist experimental limits on their branching ratios. The current values reported by the Particle Data Group [25] are $Br(\tau \rightarrow \mu\bar{\mu}\mu) < 3.2 \times 10^{-8}$ [28] and $Br(\tau \rightarrow \mu\gamma) < 4.5 \times 10^{-8}$ [29] at 90% C.L. As we will see below, these experimental limits are not enough to impose a competitive bound on $|\Omega_{\tau\mu}|$. On the other hand, the one-loop flavor violating decay $\mu \rightarrow e\gamma$, to which the τ lepton can contribute virtually inside a loop (see Figure 7), offers by far the better option to bound flavor violating transitions, as it is more strongly restricted by the experiment. The corresponding experimental limit reported by the Particle Data Group [25] is: $Br(\mu \rightarrow e\gamma) < 1.2 \times 10^{-11}$ at 90% C.L. The decay $\mu \rightarrow e\bar{e}e$ is also strongly constrained

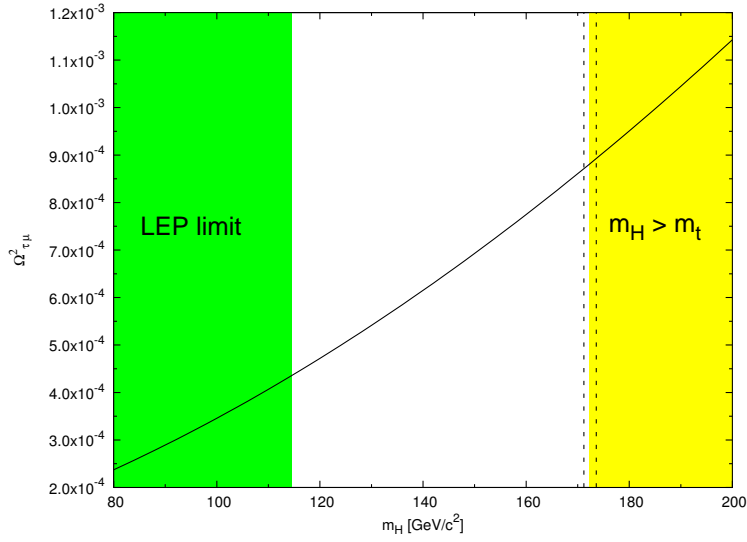


Figure 5. Behavior of $\Omega_{\tau\mu}^2$ as a function of the Higgs mass.

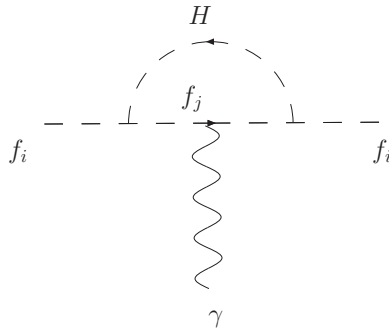


Figure 6. Diagram contributing to the magnetic and electric dipole moments of the f_i fermion.

by the experiment, but it can not be used to constraint the $H\tau\mu$ vertex at the tree level. As far as the $H\tau\mu$ contribution to the one-loop $\mu \rightarrow e\gamma$ decay, it is important to note that one needs to introduce also the $H\tau e$ coupling. Thus, it is not possible to derive directly a bound for the $\Omega_{\tau\mu}$ parameter in an isolated way, but only through the $\Omega_{\tau\mu}\Omega_{\tau e}$ product. As we will see below, a very restrictive bound on $\Omega_{\tau\mu}\Omega_{\tau e}$ can be derived, but due to the presence of the $\Omega_{\tau e}$ parameter, additional assumptions are needed in order to make predictions.

After these general considerations, we proceed to examine each of the processes above mentioned. We begin with the tree level three-body decay $\tau \rightarrow \mu\bar{\mu}\mu$, which occurs through a diagram similar to the one shown in Figure 1. Assuming a $H\mu\mu$ vertex as the one appearing in the SM, one obtains:

$$|\Omega_{\tau\mu}|^2 < \left(\frac{256\pi^2 s_W^2}{\alpha}\right) \left(\frac{m_W}{m_\mu}\right)^2 \left(\frac{\Gamma_\tau}{m_\tau}\right) \frac{Br^{Exp}(\tau \rightarrow \mu\bar{\mu}\mu)}{f(y, z)}, \quad (52)$$

where Γ_τ is total τ decay width, whereas the $f(y, z)$ function is given by Eq. (11), but

in this case $y = m_H^2/m_\tau^2$ and $z = \Gamma_H^2/m_\tau^2$. A straightforward evaluation for $m_H = 100$ GeV/ c^2 leads to

$$|\Omega_{\tau\mu}|^2 < 0.23, \quad (53)$$

which is much less restrictive than that obtained from the muon anomalous magnetic dipole moment. It is worth mentioning that an identical bound is obtained for the $\Omega_{\tau e}$ parameter using the experimental constraint on the $\tau \rightarrow e\bar{\mu}\mu$ transition, whose limit on its branching ratio is [30] $\text{Br}(\tau \rightarrow e\bar{\mu}\mu) < 3.7 \times 10^{-8}$ at 90% C.L.

We now turn to analyze the one-loop decay $l_i \rightarrow l_j\gamma$, with l_i stands for a charged lepton. The contribution of the flavor violating $Hl_i l_k$ and $Hl_k l_j$ vertices to the $l_i \rightarrow l_j\gamma$ decay is given through the diagrams shown in Figure 7. The corresponding amplitude can be written as

$$\mathcal{M}(l_i \rightarrow l_j\gamma) = \bar{u}(p_2)\Gamma_\mu u(p_1)\epsilon^{*\mu}(q, \lambda), \quad (54)$$

where the vertex function is given by

$$\Gamma_\mu = e\Omega_{ki}\Omega_{kj} \int \frac{d^D k}{(2\pi^2)^D} \sum_{a=1}^3 \frac{T_\mu^a}{\Delta_a}, \quad (55)$$

with

$$T_\mu^1 = (\not{k} + \not{p}_2 + m_k)\gamma_\mu(\not{k} + \not{p}_1 + m_k), \quad (56)$$

$$T_\mu^2 = -\frac{1}{m_i^2}(\not{k} + \not{p}_2 + m_k)(\not{p}_2 + m_i)\gamma_\mu, \quad (57)$$

$$T_\mu^3 = \frac{1}{m_i^2}\gamma_\mu\not{p}_1(\not{k} + \not{p}_1 + m_k), \quad (58)$$

$$\Delta_1 = [k^2 - m_H^2][(k + p_1)^2 - m_k^2][(k + p_2)^2 - m_k^2], \quad (59)$$

$$\Delta_2 = [k^2 - m_H^2][(k + p_2)^2 - m_k^2], \quad (60)$$

$$\Delta_3 = [k^2 - m_H^2][(k + p_1)^2 - m_k^2]. \quad (61)$$

In deriving the above expressions, a CP conserving Yukawa sector has been assumed. Also, the m_j mass has been neglected. There is no contribution to the charge, as it should be, but only to the transition magnetic dipole moment. This contribution is given by

$$\Gamma_\mu = -\frac{e\Omega_{ki}\Omega_{kj}}{32\pi^2 m_\mu} \mathcal{A} \sigma_{\mu\nu} q^\nu, \quad (62)$$

where the loop function \mathcal{A} is given by

$$\begin{aligned} \mathcal{A} = & \frac{1}{2} + m_k^2 \left(1 + \frac{m_i}{m_k}\right) C_0 + \left(\frac{m_H}{m_i}\right)^2 \left(1 - \left(\frac{m_i}{m_H}\right) \left(\frac{m_k}{m_H}\right)\right. \\ & \left. - \left(\frac{m_k}{m_H}\right)^2\right) (B_0(1) - B_0(2)). \end{aligned} \quad (63)$$

Here, $B_0(i)$ and C_0 are Passarino-Veltman scalar functions [31], which are given by $C_0 = C_0(m_i^2, 0, 0, m_H^2, m_k^2, m_k^2)$, $B_0(1) = B_0(0, m_H^2, m_k^2)$, and $B_0(2) = B_0(m_i^2, m_H^2, m_k^2)$. After squaring the amplitude, one obtains for the branching ratio:

$$\text{Br}(l_i \rightarrow l_j\gamma) = \frac{\alpha\Omega_{ki}^2\Omega_{kj}^2}{8(4\pi)^4} \left(\frac{m_i}{\Gamma_i}\right) |\mathcal{A}|^2, \quad (64)$$

where in this expression Γ_i stands for the l_i lepton decay width. This branching ratio must be less than the experimental limit, so this condition translates into a constraint for the $\Omega_{ki}\Omega_{kj}$ product,

$$|\Omega_{ki}\Omega_{kj}| < \sqrt{\frac{8(4\pi)^4}{\alpha} \left(\frac{\Gamma_i}{m_i}\right) \left(\frac{Br_{Exp}(l_i \rightarrow l_j\gamma)}{|\mathcal{A}|^2}\right)}. \quad (65)$$

To constraint $\Omega_{\tau\mu}$, we take in the above expression $l_i = l_k = \tau$ and $l_j = \mu$, with the $H\tau\tau$ coupling as in the SM. Once introduced these changes in the above general result, one obtains

$$|\Omega_{\tau\mu}| < \frac{64\pi s_W}{\alpha} \left(\frac{m_W}{m_\tau}\right) \sqrt{\frac{\pi}{2} \left(\frac{\Gamma_\tau}{m_\tau}\right) \left(\frac{Br_{Exp}(\tau \rightarrow \mu\gamma)}{|\mathcal{A}|^2}\right)}, \quad (66)$$

which ($m_H = 100 \text{ GeV}/c^2$) leads to the following constraint:

$$|\Omega_{\tau\mu}| < 10^{-1}, \quad (67)$$

which is about one order of magnitude less stringent than that obtained from the muon magnetic dipole moment.

Although it is not possible to obtain an acceptable constraint for the $\Omega_{\tau\mu}$ parameter, it is interesting to analyze the constraint induced by the experimental limit on the $\mu \rightarrow e\gamma$ decay on the $|\Omega_{\tau\mu}\Omega_{\tau e}|$ product. In Figure 8, its behavior as a function of m_H is displayed. For clarity, this variation is shown for m_H ranging from 80 to 200 GeV/c^2 . It can be appreciated from this figure that $|\Omega_{\tau\mu}\Omega_{\tau e}|$ varies in this interval from approximately 1.5×10^{-7} to 8×10^{-7} . Although very stringent, this constraint cannot be used to predict the $H\tau\mu$ vertex without making additional assumptions concerning the $\Omega_{\tau e}$ parameter. However, if we adopt an approach similar to the one used for the $\Omega_{tu}\Omega_{tc}$ product, a very restrictive branching ratio for the $t \rightarrow u_i\tau l_i$ decay is obtained, as the corresponding bound for $\Omega_{\tau l_i}$ ($l_i = e, \mu$) is more stringent than that obtained from the muon anomalous magnetic moment by more than two orders of magnitude. Although we prefer to make predictions for the $t \rightarrow u_i\tau\mu$ transition using the constraint for $\Omega_{\tau\mu}$ obtained from the muon magnetic moment, as it does not require of introducing extra assumptions, the scenario for a very constrained $t \rightarrow u_i\tau l_i$ decay will be also discussed. Indeed, this is a good approach to predict the branching ratio of the $t \rightarrow u_i\tau e$ transition but not for the $t \rightarrow u_i\tau\mu$, as it is natural to expect that $\Omega_{\tau\mu} > \Omega_{\tau e}$. The possibility of considering some type of relations between the $\Omega_{\tau\mu}$ and $\Omega_{\tau e}$ parameters will be not considered in this work because, as it is emphasized in the introduction, our study will be supported only in the available experimental data. On the other hand, it should be commented that a similar analysis to the presented here was carried out some years ago [32] to constraint the λ_{ij} parameters appearing in the Cheng-Sher ansatz within the context of multi-Higgs extensions of the SM. We have verified that our results are in perfect agreement with those given in this reference.

To finish this section, it is interesting to compare our bound for $\Omega_{\tau\mu}$ with than that can be derived from the Cheng-Sher ansatz. In this case, $\Omega_{\tau\mu} < \sqrt{m_\tau m_\mu}/v \approx 1.7 \times 10^{-3}$, which shows that our bound obtained from the muon anomalous magnetic dipole moment is less restrictive by about one order of magnitude.

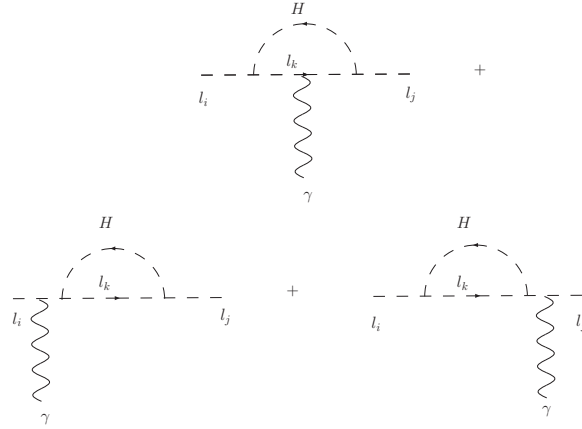


Figure 7. Diagrams contributing to the $l_i \rightarrow l_j \gamma$ decay.

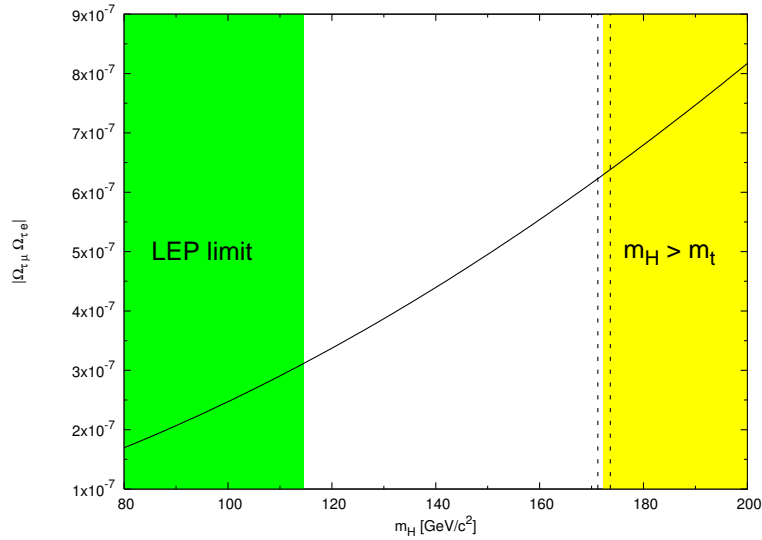


Figure 8. Allowed values for the product $|\Omega_{\tau\mu}\Omega_{\mu e}|$ as a function of the Higgs mass.

5. Results and discussion

In this section, we discuss our results. As commented at the end of the previous section, we will discuss the branching ratio of the $t \rightarrow u_i \tau \mu$ decay using the constraint for the $H\tau\mu$ vertex obtained from the muon anomalous magnetic moment, and also for the branching ratio of the $t \rightarrow u_i l_i$ transition using a bound for the $H\tau l_i$ coupling derived from the experimental limit on the $\mu \rightarrow e\gamma$ decay. In the latter case, our result is a good prediction for the $t \rightarrow u_i \tau e$ decay, but not for the $t \rightarrow u_i \tau \mu$ one, as it is natural to assume that the $\Omega_{\tau\mu} > \Omega_{\tau e}$ relation is satisfied in the fundamental theory.

5.1. Decay $t \rightarrow u_i \tau \mu$

When the $t \rightarrow u_i \tau \mu$ transition is mediated by the H scalar resonance, the highest value that can reach the corresponding branching ratio can be expressed simply as

$$Br(t \rightarrow u_i \tau \mu) = Br(t \rightarrow u_i H) Br(H \rightarrow \tau \mu), \quad (68)$$

where

$$Br(t \rightarrow u_i H) = \frac{\Omega_{tu}^2}{32\pi} \left(\frac{m_t}{\Gamma_t} \right) \left(1 - \left(\frac{m_H}{m_t} \right)^2 \right)^2 \quad (69)$$

$$Br(H \rightarrow \tau \mu) = \frac{\Omega_{\tau\mu}^2}{4\pi} \left(\frac{m_H}{\Gamma_H} \right) \left(1 - \left(\frac{m_\tau}{m_H} \right)^2 \right)^2 \quad (70)$$

In writing these expressions we have ignored the u_i and μ masses. These branching ratios are of interest by themselves, so we will evaluate them for an allowed value of the Higgs mass that maximize their values. As it can be seen from Figure 10, the branching ratio for the decay $t \rightarrow u_i \tau \mu$ reach its highest value around $m_H = 105 \text{ GeV}/c^2$, that is below the region allowed for the present analysis ($114.4 \text{ GeV}/c^2 < m_H < 171.3 (\pm 1.1) \text{ GeV}/c^2$). Specifically, to estimate these branching ratios, we will take $m_H = 115 \text{ GeV}/c^2$. In addition, we will use for the total top decay width the approximation $\Gamma_t \approx \Gamma(t \rightarrow bW) = 1.55 \text{ GeV}/c^2$. Using these values and the constraint $\Omega_{tu}^2 < 1.03 \times 10^{-3}$ derived from Eq. (26), one obtains $Br(t \rightarrow H u_i) \sim 3.7 \times 10^{-4}$. As far as $Br(H \rightarrow \tau \mu)$ is concerned, we will use the constraint $\Omega_{\tau\mu}^2 < 2 \times 10^{-4}$ and a total Higgs decay width given by: $\Gamma_H = \Gamma(H \rightarrow \text{all SM decay modes}) + \Gamma(H \rightarrow \tau \mu) + \Gamma(H \rightarrow \tau l_i)$. In Fig. 9, the behavior of the branching ratios for the $H \rightarrow \tau \mu$ and $H \rightarrow \tau l_i$ decays are shown as a function of the Higgs mass. In order to appreciate their relative importance, the branching ratios associated with the most representative SM Higgs decays are shown too. It can be appreciated from this figure that $Br(H \rightarrow \tau \mu)$ ranges from 0.37 to 0.04 in the interval $115 \text{ GeV} < m_H < 2m_W$. In this way, the branching ratio for the $t \rightarrow u_i \tau \mu$ decay can reach the value 1.37×10^{-4} , at the best.

Before discussing our result for the branching ratio of the $t \rightarrow u_i \tau \mu$ decay, it is worth comparing our prediction for the two-body $t \rightarrow u_i H$ and $H \rightarrow \tau \mu$ decays with those found in other contexts. We will focus on the rare top decay $t \rightarrow cH$, as the $t \rightarrow uH$ mode is expected to be much more suppressed. In the SM, this decay is quite suppressed to be detected, as it has a branching ratio ranging from 10^{-13} to 10^{-14} for $m_Z < m_H < 2m_W$ [4]. Although very suppressed in the SM, this decay can reach sizable branching ratios in many well-motivated SM extensions. For instance, it can reach branching ratios ranging from 10^{-3} to 10^{-7} in the general two-Higgs doublet models [34] or in the minimal supersymmetric standard model [35]. As the lepton flavor violating Higgs decays is concerned, they are absent at any order of perturbation theory in the SM, but they can be induced with sizable branching ratios in many of its extensions. For instance, the decay $H \rightarrow \tau \mu$ can reach branching ratios as large as $10^{-3} - 10^{-2}$ in the THDM-III [36], in the MSSM [37], or in a specific SUSY- $SU(5)$ scenario [11]. Motivated by the strong experimental evidence of nonzero masses for the light neutrinos [38], important attention has received the possible violation of the lepton flavor mediated by the Higgs boson in the context of seesaw models. Although these decays are very suppressed within the SM-seesaw model [39, 40], with branching

|| The total decay width for all SM-Higgs decay modes was evaluated using the current version of the HDECAY program [33].

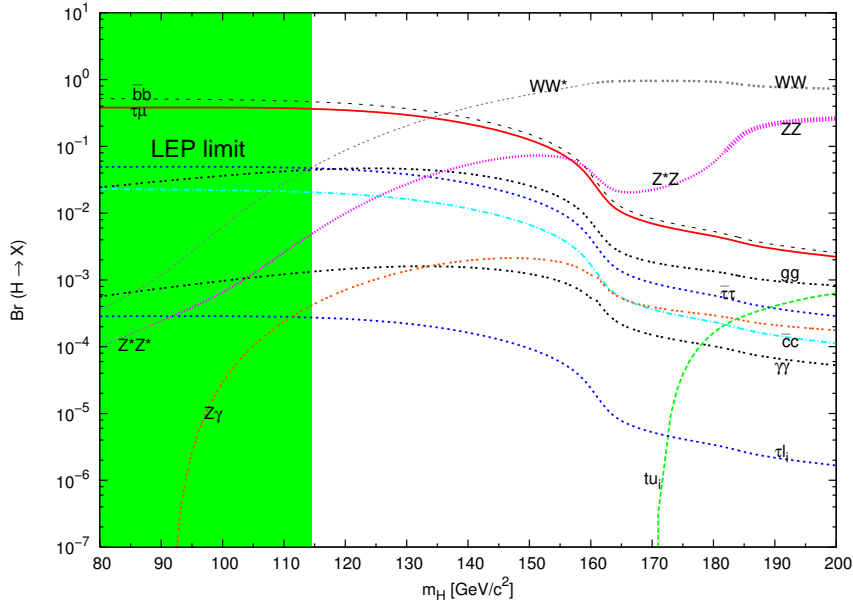


Figure 9. Branching ratios for the Higgs boson decay into the $\bar{b}b$, $\bar{\tau}\tau$, $\bar{c}c$, gg , $Z\gamma$, WW^* , WW , Z^*Z^* , Z^*Z , ZZ , $\tau\mu$, τl_i , and tu_i modes as a function of m_H .

ratios of order of 10^{-56} , they can dramatically be enhanced in other models, as the MSSM-seesaw model, in which can reach values as large as 10^{-5} [40].

We now turn to discuss the branching ratio for the $t \rightarrow u_i \tau \mu$ decay. As it can be appreciated from Figure 10, this branching ratio reach its highest value of approximately 10^{-4} for $m_H = 105$ GeV/ c^2 , but we are interested in examining its behavior for values of m_H above the LEP limit. It can be seen from this figure that for $115 < m_H < 2m_W$, $Br(t \rightarrow u_i \tau \mu)$ varies from approximately 10^{-4} to 10^{-5} . However, the branching ratio decreases strongly for $m_H > 2m_W$, which means that this decay is only interesting when mediated by a relatively light Higgs boson. The importance of this branching ratio can be best appreciated if compared with those existing in the literature for other top quark three-body decays. In the SM, the three-body decays of the top quark are in general very suppressed. For instance, the flavor violating decays $t \rightarrow cWW$ [1], $t \rightarrow u_i \bar{u}_j u_j$ [41, 42], and $t \rightarrow cgg$ [42] have branching ratios of order of 10^{-12} , 3.4×10^{-12} , and 10^{-9} , respectively. Interestingly, it was found [41, 42] that the latter two decays have branching ratios as large as or larger than those associated with the two-body decay $t \rightarrow u_i g$ [3]. However, the decays $t \rightarrow cV_i V_j$ ($V_i = W, Z, \gamma, g$) can have sizable branching ratios of order of 10^{-4} to 10^{-6} in the THDM [43] and the MSSM [44]. On the other hand, branching ratios of order of $10^{-8} - 10^{-5}$ has been determined in the context of the THDM-III [45, 46] and the MSSM [46] for the quark flavor violating, but lepton flavor conserving, $t \rightarrow cl^+ l^-$ decay. The double flavor violating $t \rightarrow u_i \tau \mu$ decay has thus an important branching ratio within this category of rare top quark decays.

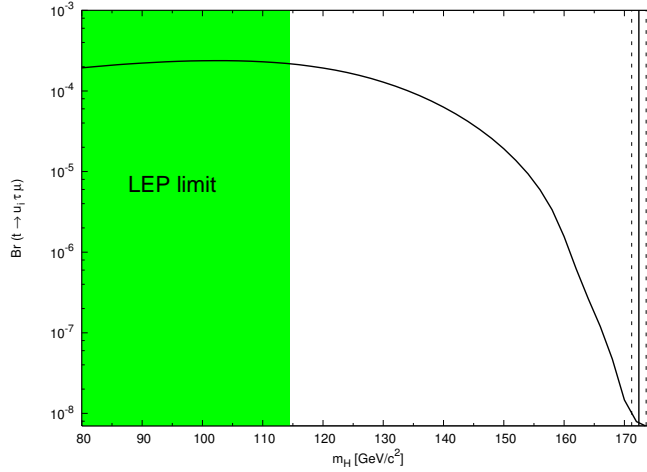


Figure 10. Branching ratio for the $t \rightarrow u_i \tau \mu$ decay as a function of the Higgs mass.

5.2. Decay $t \rightarrow u_i \tau l_i$

This subsection is devoted to discuss the branching ratio for the $t \rightarrow u_i \tau l_i$ decay using the constraint for the $H \tau l_i$ vertex derived from the experimental limit on the $\mu \rightarrow e \gamma$ transition. As mentioned at the end of the previous section, our result is a good prediction for the $t \rightarrow u_i \tau e$ decay, but not for the $t \rightarrow u_i \tau \mu$ one, as it is expected that the $H \tau e$ vertex is much more suppressed than the $H \tau \mu$ one. The behavior of $Br(H \rightarrow \tau l_i)$ as a function of the Higgs mass is shown in Fig. 9. From this figure, it can be appreciated that this branching ratio ranges from 2.7×10^{-4} to 3.1×10^{-5} for a Higgs mass in the interval $115 \text{ GeV} < m_H < 2m_W$. Using the bound for $Br(t \rightarrow u_i H)$ derived from the $D^0 - \bar{D}^0$ mixing, it is found that $Br(t \rightarrow u_i \tau l_i) = 1.05 \times 10^{-7}$, at the best. Its behavior as a function of the Higgs mass is shown in Fig. 11. Strictly speaking, this result can be considered as a stringent bound for the $t \rightarrow u \tau e$ decay, in whose derivation the conservative point of view of assuming $\Omega_{tc} = \Omega_{tu}$ and $\Omega_{\tau\mu} = \Omega_{\tau e}$ was adopted. This branching ratio is too much small to be at the reach of the LHC sensitivity.

5.3. Experimental perspectives

The Large Hadron Collider will be an ideal machine for investigating the characteristic of the heaviest quark and its role in the SM. With a NLO production cross-section of about 830 pb , two top-pairs per second are expected to be produced. This means that we should be able to collect more than 10 millions of $t\bar{t}$ per year at low luminosity conditions of around $2 \times 10^{33} \text{ cm}^2 \text{ s}^{-1}$. The $t\bar{t}$ production at the LHC is predicted to take place via two distinct hard processes, the $gg \rightarrow t\bar{t}$, which will contribute for about 90% to the total production cross section and $g\bar{q} \rightarrow t\bar{t}$ process which contributes for the remaining 10%.

Within the SM, a top, with a mass above Wb threshold, is predicted to have a decay width dominated by the two-body process: $t \rightarrow Wb$ ($Br \simeq 0.998$) [25]. A $t\bar{t}$ pair will then decay via one of the following channels, classified according to the final states: *i*) dilepton, where both W decays are leptonic (ℓ_W), with 2 jets arising from the

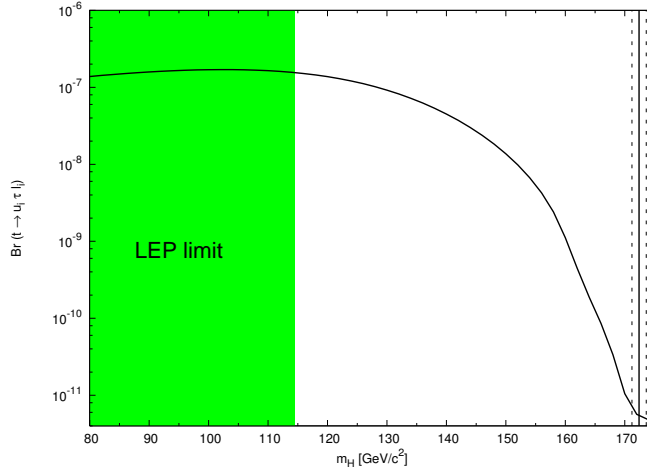


Figure 11. Branching ratio for the $t \rightarrow u_i \tau l_i$ decay as a function of the Higgs mass.

two b -quark hadronization and missing transverse energy (\cancel{E}_T) [47] coming from the undetected neutrinos: $Br(e, e) = Br(\mu, \mu) = Br(\tau, \tau) \simeq 1/81$, $Br(e, \mu) = Br(e, \tau) = Br(\mu, \tau) \simeq 2/81$; ii) lepton + jets, where one W decays leptonically and the other one into quarks, with 4 jets and \cancel{E}_T : $Br(e + jets) = Br(\mu + jets) = Br(\tau + jets) \simeq 12/81$; iii) all jets, where both the W 's decay into quarks with 6 jets and no associated \cancel{E}_T ; the corresponding branching fraction is $Br(jets) \simeq 36/81$.

If \mathcal{B} represents the branching ratio for the Higgs mediated double flavor violating top quark decay: $\mathcal{B} \equiv Br(t \rightarrow u_i \tau \mu)$ and if we assume no other significantly accessible decay channels, either than the SM and the DFV, we will have: $Br(t \rightarrow Wb) = 1 - \mathcal{B}$. A $t\bar{t}$ pair can then decays as follows: a) purely SM decays (SM-SM), where both the top quarks decay into Wb ($Br(t\bar{t})|_{SM} = (1 - \mathcal{B})^2$); b) mixed SM-DFV decays, where one top will decay into Wb and the other into $u_i \mu \tau$ ($Br(t\bar{t})|_{SM-DFV} = 2\mathcal{B}(1 - \mathcal{B})$); c) purely DFV decays (DFV-DFV), in this case both the top quarks will decay into $u_i \mu \tau$ ($Br(t\bar{t})|_{DFV} = \mathcal{B}^2$). As a purely DFV $t\bar{t}$ decay is strongly suppressed ($\mathcal{B} \simeq 10^{-6} - 10^{-8}$), we will focus only on SM-DFV top quark decays.

The τ leptons, produced by the DFV top quark, will decay either in $e\bar{\nu}_e\nu_\tau$ or $\mu\bar{\nu}_\mu\nu_\tau$ (τ_ℓ) or to hadrons (τ_h). The branching ratios for such decay processes are: $\Gamma^\tau(\mu\bar{\nu}_\mu\nu_\tau)/\Gamma_{Total}^\tau = 0.1736 \pm 0.005$, $\Gamma^\tau(e\bar{\nu}_e\nu_\tau)/\Gamma_{Total}^\tau = 0.1784 \pm 0.005$ and $\Gamma^\tau(\tau \rightarrow jet)/\Gamma_{Total}^\tau \simeq 0.653$ [25]. In $\simeq 77\%$ of hadronic τ decays, only one charged track is produced: $\tau \rightarrow \nu_\tau + 3\pi^\pm + n\pi^0$ (1-prong decay); in the other $\simeq 23\%$ of cases we will have 3 charged tracks: $\tau \rightarrow \nu_\tau + 3\pi^\pm + n\pi^0$ (3-prong decay). A τ lepton, decaying hadronically, will generate a small jet (τ_h) with hadrons and neutrinos amongst the decay products. The presence of such a particles makes difficult to reconstruct and identify efficiently the τ -jets. The background misidentified as a τ_h is mainly QCD multi jet events, but also electrons that shower late or with strong bremsstrahlung, or muons interacting in the calorimeters. When the momentum of the τ is large, compared to the mass, a very collimated jet will be produced. Then, a τ -jet can be identified through the presence of a well collimated calorimeter cluster with a small number of associated charged tracks (1 to 3). At LHC center of mass energy, for a transverse momentum $P_T > 50$ GeV/c, 90% of the energy is contained

in a cone of radius $R = \sqrt{\Delta\eta^2 + \Delta\Phi^2} = 0.2$. Hadronic τ decays have low charged track multiplicity and a relevant fraction of electromagnetic energy deposition in the calorimeters due to photons coming from the decay of neutral pions.

As in the channel $t\bar{t} \rightarrow u_i\tau\mu Wb$ there is no charge correlation between the μ and the W , coming from the top decay, if the W decays leptonically ($W \rightarrow \ell\nu_\ell$) it is possible to have both like-sign (LS) and opposite-sign (OS) μ - e final states: $\mu^\pm e^\pm$ and $\mu^\pm e^\mp$. In order to be able to reconstruct the top, decaying via DFV processes, we will look only for final states containing an electron, a muon and a jet, identified as coming from a hadronic tau decay (τ -jet), a jet identified as coming from a b quark (b -jet), and a certain number of jets produced by the u_i ($u_i = u, c$) hadronization and from the initial (ISR) and final state radiation (FSR). Because of the presence of neutrinos in the final states, we will also require to have missing transverse energy in the detector. The experimental signature adopted, in the present analysis, is then the following tri-lepton final state: $e\mu^\pm\tau_h^\mp + \cancel{E}_T + b + \text{jets}$.

As the cross section, for the channel under study, ranges, for $\sqrt{s} = 1.96$ TeV, between 1.4 fb and 0.1 fb, for a Higgs mass between 114.4 and 165 GeV/ c^2 , Higgs mediated double flavor violating top quark decays are out of reach of Tevatron experiments.

Higgs mediated DFV top quark decays and SM background events have been generated using the PYTHIA 8.108 Montecarlo program. Initial and final-state radiation, hadronization and decay have been included. Jets have been reconstructed using the GETJET cone algorithm and a toy Montecarlo simulation of the detector effect efficiencies have been included in the calculations. Events have been selected by applying the following set of cuts. The presence of a central, isolated, high- P_T muon with $P_T^\mu > 20$ GeV/ c and $|\eta_\mu| < 2.4$ [47]. The presence of a central, isolated, high- P_T , hadronically decayed, τ , tagged as a τ -jet [48] with $P_T^\tau > 20$ GeV/ c and $|\eta_\tau| < 2.4$. Jets are reconstructed with a cone size of $R = \sqrt{(\Delta\eta)^2 + (\Delta\phi)^2} = 0.5$ and the events are required to have at least two jets with a trasverse energy of $E_T^{\text{jet}} > 30$ GeV within a fiducial volume of $|\eta_{\text{jet}}| < 2.4$ (here the τ 's are not counted as jets). Because of the presence of neutrinos in the final state, the missing transverse energy is required to be: $\cancel{E}_T > 60$ GeV and the μ and the τ are asked to have opposite sign. The events are then required to have a jet tagged as a b and to have a central, isolated, high- P_T electron with $P_T^e > 20$ GeV/ c and $|\eta_e| < 2.4$. A further cut, on the reconstructed transverse mass $M_T(\mu, \tau, j)$ of the muon, the tau and the jet, with the highest P_T , not tagged as a b -jet, is applied in order do discriminate the signal from the SM backgrounds.

The SM backgrounds, considered in the present analysis, include $t\bar{t}$ events, ZZ +jets, WW +jets, ZW +jets and $Z+\gamma$ with the γ that later converts in the detector giving a lepton pair.

The Large Hadron Collider, will start to operate soon delivering the first proton proton collisions. The luminosity will be ramping from initial 3×10^{28} to about 2×10^{31} cm $^{-2}$ s $^{-1}$, within first months of LHC commissioning. In the second phase of LHC operation (within 1-2 years), the luminosity should achieve the designed value of 10^{34} cm $^{-2}$ s $^{-1}$ with a bunch crossing time of 25 ns. In total, an integrated luminosity of 300 fb $^{-1}$ should be collected, within the first 5 years of LHC operation and about 700 fb $^{-1}$ before the phase two of the upgrade. In total, the integrated luminosity delivered, in course of LHC and SLHC running, is expected to reach a value of about 3000 fb $^{-1}$ [49]. In the scenario considered here, it will be possible, by using a total integrated luminosity of 3000 fb $^{-1}$ of data, to rule out, at 95 % C.L., Double Flavor

Violating top quark decays, mediated by a Higgs, with a mass up to 155 GeV/ c^2 or discover this process for a Higgs up to 147 GeV/ c^2 .

6. Conclusions

The quark top and the Higgs boson, would constitute the heaviest particles living at the Fermi scale. Therefore, these particles would play an important role in flavor violating transitions, as the mass seems to be intimately related with this class of physics effects. It is thus expected that the large masses of these particles tend to favor flavor violating transitions both in the quark sector and in the lepton sector. Apart from the large masses of these particles, the prospects of detecting this class of new physics effects are reinforced by the very peculiar dynamic behavior of the top quark and the strong evidence of nonzero neutrino mass that naturally leads to lepton flavor violating transitions mediated by the Higgs boson. Under these circumstances, Higgs-mediated double flavor violating transitions of the top quark could be at the reach of the next colliders. In this paper, this possibility has been explored in a model-independent manner using the effective Lagrangian approach. A Yukawa sector that includes all the $SU_L(2) \times U_Y(1)$ -invariant operators of up to dimension six was proposed and used to construct the most general renormalizable flavor violating $q_i q_j H$ and $H l_i l_j$ vertices. Low-energy data were used to constraint the $t u_i H$ and $H \tau \mu$ couplings and then used to predict the double flavor violating decay $t \rightarrow u_i \tau \mu$. It was found that this decay has a branching ratio of order of $10^{-4} - 10^{-5}$ for a relatively light Higgs boson with mass in the range $115 \text{ GeV}/c^2 < m_H < 2m_W$. Such kind of decays are out of the reach of Tevatron experiments. Considering that LHC will operate as a veritable top quark factory, by studying the following final state: $e \mu^\pm \tau_h^\mp + \cancel{E}_T + b + \text{jets}$ and by using a total integrated luminosity of 3000 fb^{-1} , it will be possible to rule out, at 95% C.L., DFV top quark decays up to a Higgs mass of 155 GeV/ c^2 or discover such a process up to a Higgs mass of 147 GeV/ c^2 .

Acknowledgments

We thank CONACYT (México), the HELEN ALFA-EC program and the Università di Cassino (Italy) for their financial support.

- [1] Elizabeth Jenkins, Phys. Rev. **D56**, 458 (1997).
- [2] R. Decker, M. Nowakowski, and A. Pilaftsis, Z. Phys. **C57**, 339 (1993); G. Mahlon and S. J. Parke, Phys. Lett. **B347**, 394 (1995); S. Eidelman *et al.*, Phys. Lett. **B592**, 1 (2004).
- [3] G. Eilam, J. L. Hewett, and A. Soni, Phys. Rev. **D44**, 1473 (1991); **59**, 039901(E) (1999); J. L. Díaz-Cruz, R. Martínez, M. A. Pérez, and A. Rosado, Phys. Rev. **D41**, 891 (1990).
- [4] B. Mele and S. Petrarca, Phys. Lett. **B435**, 401 (1998).
- [5] F. Abe *et al.*, Phys. Rev. **D51**, 4623 (1995); Phys. Rev. Lett. **79**, 1992 (1997); **79**, 3585 (1997); **80**, 2525 (1998); **80**, 2767 (1998); **80**, 2773 (1998); **80**, 2779 (1998); **80**, 5720 (1998); **82**, 271 (1999); S. Abachi *et al.*, *ibid.* **79**, 1197 (1997); **79**, 1203 (1997); B. Abbott *et al.*, *ibid.* **80**, 2063 (1998); **83**, 1908 (1999); Phys. Rev. **D58**, 052001 (1998); T. Affolder *et al.*, Phys. Rev. Lett. **84**, 216 (2000).
- [6] For a review on top quark physics, see D. Chakraborty, J. Konigsberg, and D. Rainwater, Annu. Rev. Nucl. Part. Sci. **53**, 301 (2003). See also M. Beneke *et al.*, hep-ph/0003033; F. Larios, R. Martínez, and M. A. Pérez, Phys. Rev. **D72**, 057504 (2005); Int. J. Mod. Phys. **A21**, 3473 (2006).
- [7] See for instance, Z. Hioki, hep-ph/0407319.

- [8] F. Abe *et al.* (CDF Collaboration), Phys. Rev. Lett. **80**, 2779 (1998); D. Acosta *et al.* (CDF Collaboration), Phys. Rev. Lett. **93**, 142001 (2004); CDF Collaboration, http://www-cdf.fnal.gov/physics/new/top/public_xsection.html - Conf. Note 9890.
- [9] W. Buchmuller and D. Wyler, Nucl. Phys. **B268**, 621 (1986). See also, J. Wudka, Int. J. Mod. Phys. **A9**, 2301 (1994).
- [10] Adriana Cordero-Cid, M. A. Pérez, G. Tavares-Velasco, and J. J. Toscano, Phys. Rev. **D70**, 074003 (2004).
- [11] J. Lorenzo Díaz-Cruz and J. J. Toscano, Phys. Rev. **D62**, 116005 (2000). See also, A. Flores-Tlalpa, J. M. Hernández, G. Tavares-Velasco, and J. J. Toscano, Phys. Rev. **D65**, 073010 (2002).
- [12] F. del Aguila, M. Pérez-Victoria, and J. Santiago, Phys. Lett. **B492**, 98 (2000).
- [13] B. Aubert *et al.* (BaBar Collaboration), Phys. Rev. Lett. **98**, 211802 (2007).
- [14] M. Starič *et al.* (Belle Collaboration), Phys. Rev. Lett. **98**, 211803 (2007)
- [15] Heavy Flavor Averaging Group, <http://www.slac.stanford.edu/xorg/hfag/index>.
- [16] Higgs-mediated lepton flavor violating transitions are analyzed in: Adriana Cordero-Cid, G. Tavares-Velasco, and J. J. Toscano, Phys. Rev. **D72**, 117701 (2005); J. I. Aranda, F. Ramírez-Zavaleta, J. J. Toscano, and E. S. Tututi, Phys. Rev. **D78**, 017302 (2008).
- [17] C. Arzt, M. B. Einhorn, and J. Wudka, Nucl. Phys. **B433**, 41 (1995).
- [18] See for instance, J. L. Díaz-Cruz, R. Noriega-Papaqui, and A. Rosado, Phys. Rev. **D69**, 095002 (2004); Phys. Rev. **D71**, 015014 (2005).
- [19] J. L. Feng, T. Moroi, H. Murayama, and E. Schnapka, Phys. Rev. **D57**, 5875 (1998).
- [20] I. Dorsner and S. M. Barr, Phys. Rev. **D65**, 095004 (2002).
- [21] T. P. Cheng and M. Sher, Phys. Rev. **D35**, 3484 (1987).
- [22] The impact of new physics on $D^0 - \bar{D}^0$ mixing is analyzed in diverse contexts in: E. Golowich, J. Hewett, S. Pakvasa, and A. A. Petrov, Phys. Rev. **D76**, 095009 (2007).
- [23] M. Artuso *et al.* (CLEO Collaboration), Phys. Rev. Lett. **95**, 251801 (2005).
- [24] R. Gupta, T. Bhattacharya, and S. R. Sharpe, Phys. Rev. **D55**, 4036 (1977).
- [25] C. Amsler *et al.* (Particle Data Group), Phys. Lett. **B667**, 1 (2008).
- [26] The most recent bound on d_n is reported in: C. A. Baker *et al.*, Phys. Rev. Lett. **97**, 131801 (2006).
- [27] C. Pagliarone, A. Fernández, and J. J. Toscano, arXiv:0802.1949 [hep-ph].
- [28] Y. Miyazaki *et al.* (Belle Collaboration), Phys. Lett. B **660**, 154 (2008).
- [29] K. Hayasaka *et al.* (Belle Collaboration), Phys. Lett. B **666**, 16 (2008).
- [30] B. Aubert *et al.* (The Babar Collaboration), Phys. Rev. Lett. **99**, 251803 (2007).
- [31] G. Passarino and M. J. G. Veltman, Nucl. Phys. **B160**, 151 (1979).
- [32] M. Sher and Y. Yuan, Phys. Rev. **D44**, 1461 (1991).
- [33] A. Djouadi, J. Kalinowski and M. Spira, Comput. Phys. Commun. **108**, 56 (1998).
- [34] W. S. Hou, Phys. Lett. **B296**, 179 (1992); J. A. Aguilar-Saavedra and G. C. Branco, Phys. Lett. **B495**, 347 (2000); E. O. Iltan, Phys. Rev. **D65**, 075017 (2002); S. Béjar, J. Guasch, and J. Solà, Nucl. Phys. **B675**, 270 (2003).
- [35] J. M. Yang and C. S. Li, Phys. Rev. **D49**, 3412 (1994), **51**, 3974 (1995) (E); J. Guasch and J. Solà, Nucl. Phys. **B562**, 3 (1999); G. Eilam, A. Gemintern, T. Han, J. M. Yang, and X. Zhang, Phys. Lett. **B510**, 227 (2001).
- [36] S. Kanemura, T. Ota, and K. Tsumura, Phys. Rev. **D73**, 016006 (2006).
- [37] S. Kanemura, K. Matsuda, T. Ota, T. Shindou, E. Takasugi, and K. Tsumura, Phys. Lett. **B599**, 83 (2004).
- [38] Y. Fukuda *et al.*, Phys. Rev. Lett. **77**, 1683 (1996); V. N. Gavrin, Nucl. Phys. Proc. Suppl. **91**, 36 (2001); W. Hampel *et al.*, Phys. Lett. **B447**, 127 (1999); M. Altmann *et al.*, Phys. Lett. **B490**, 16 (2000); S. Fukuda *et al.*, Phys. Rev. Lett. **86**, 5651 (2001); **86**, 5656 (2001); Q. R. Ahmad *et al.*, Phys. Rev. Lett. **87**, 071301 (2001); **89**, 011302 (2002); K. Eguchi *et al.*, Phys. Rev. Lett. **90**, 021802 (2003).
- [39] A. Pilaftsis, Z. Phys. **C55**, 275 (1992); Phys. Lett. **B285**, 68 (1992); J. G. Körner, A. Pilaftsis, and K. Schilcher, Phys. Rev. **D47**, 1080 (1993).
- [40] E. Arganda, A. M. Curiel, M. J. Herrero, and D. Temes, Phys. Rev. **D71**, 035011 (2005).
- [41] A. Cordero-Cid, J.M. Hernández, G. Tavares-Velasco, and J. J. Toscano, Phys. Rev. **D73**, 094005 (2006).
- [42] G. Eilam, M. Frank, and I. Turan, Phys. Rev. **D73**, 053011 (2006).
- [43] S. Bar-Shalom, G. Eilam, A. Soni, and J. Wudka, Phys. Rev. Lett. **79**, 1217 (1997); Phys. Rev. **D57**, 2957 (1998); J. L. Díaz-Cruz, M. A. Pérez, G. Tavares-Velasco, and J. J. Toscano, Phys. Rev. **D60**, 115014 (1999); S. Bar-Shalom, G. Eilam, M. Frank, and I. Turan, Phys. Rev. **D72**, 055018 (2005).

- [44] J. J. Cao, G. Eilam, M. Frank, K. Hikasa, G. L. Liu, I. Turan, and J. M. Yang, Phys. Rev. **D75**, 075021 (2007).
- [45] E. O. Iltan and I. Turan, Phys. Rev. **D67**, 015004 (2003).
- [46] Mariana Frank and I. Turan, Phys. Rev. **D74**, 073014 (2006).
- [47] We use a (z, ϕ, θ) coordinate system where the z -axis is in the direction of the proton beam, and ϕ and θ are the azimuthal and polar angles respectively. The pseudo-rapidity, η , is defined as $-\ln(\tan \frac{\theta}{2})$. The transverse momentum of a charged particle is $P_T = P \sin \theta$, where P represents the measured momentum of the charged-particle track. The analogous quantity using calorimeter energies, defined as $E_T = E \sin \theta$ is called transverse energy. The missing transverse energy is defined as $\cancel{E}_T = - | \sum_i E_T^i \hat{n}_i |$ where E_T^i is the magnitude of the transverse energy contained in each calorimeter tower i in the pseudo-rapidity region $|\eta| < 3.6$ and \hat{n}_i is the direction unit vector of the tower in the plane transverse to the beam direction.
- [48] G. Bagliesi, arXiv:0707.0928 [hep-ex].
- [49] P. Sicho, Nucl. Instrum. Meth. A **607**, 31 (2009).